

Monthly Gridded Geopotential Height and Temperature from Global Positioning System (GPS) Radio Occultation (RO)

1. Intent of This Document and POC

1a) This document is intended for users who wish to compare satellite derived observations with climate model output in the context of the CMIP5/IPCC historical experiments. Users are not expected to be experts in satellite derived Earth system observational data. This document summarizes essential information needed for comparing this dataset to climate model output. References are provided at the end of this document to additional information.

This NASA dataset is provided as part of an experimental activity to increase the usability of NASA satellite observational data for the modeling and model analysis communities. This is not a standard NASA satellite instrument product, but does represent an effort on behalf of data experts to identify a product that is appropriate for routine model evaluation. The data may have been reprocessed, reformatted, or created solely for comparisons with climate model output. Community feedback to improve and validate the dataset for modeling usage is appreciated. Email comments to HQ-CLIMATE-OBS@mail.nasa.gov.

Dataset File Name (as it appears on the ESGF):

ta_RO_L3_Ret-v1.3_200201-201412.nc

zg_RO_L3_Ret-v1.3_200201-201412.nc

1b) Technical point of contact for this dataset:

Chi O. Ao, chi.o.ao@jpl.nasa.gov

2. Data Field Description

CF variable name, units:	zg in meters; ta in Kelvins
Spatial resolution:	5 deg x 5 deg at pressure levels (400, 375, 350, 325, 300, 275, 250, 225, 200, 170, 150, 130, 115, 110, 100, 90, 80, 70, 50, 40, 30, 20, 15, 10) hPa
Temporal resolution and extent:	Monthly averaged, from 01/2002 to 12/2014
Coverage:	Global

3. Data Origin

This dataset comes from a combination of the CHAMP (CHAllenging Minisatellite Payload) [Wickert et al. 2001] and COSMIC (Constellation Observing System for Meteorology, Ionosphere, and Climate, also known as FORMOSAT-3) [Anthes et al. 2008] measurements, with CHAMP observations covering the period of January 2002 to April 2006 and COSMIC observations covering the period of May 2006 to

December 2014. The CHAMP RO mission consists of a single spacecraft with an aft-viewing RO antenna capable of producing about 200 globally distributed profiles per day. The COSMIC RO mission consists of multiple spacecraft with both aft and fore antenna capable of observing up to about 2000 profiles per day.

The raw data are processed at JPL using the GPS Occultation Analysis Software (GOAS) [Hajj et al., 2002]. The retrieved bending angle, refractivity, and temperature profiles can be accessed through the GENESIS web portal (<http://genesis.jpl.nasa.gov>). To obtain the monthly gridded data at each pressure level, we apply the Bayesian mapping technique whereby the data are optimally fitted with a set of spherical harmonic basis functions. Fig. 1 illustrates the Bayesian mapping method applied to 5 days of geopotential height data at 200 hPa from CHAMP and COSMIC. The optimal number of spherical harmonics varies depending on sampling density. Our study showed that spherical harmonics up to a maximum degrees of 14 and 18 worked well for CHAMP and COSMIC, respectively [Leroy et al., 2012]. The values at any specified latitude and longitude can be quickly computed using the fitting coefficients. The fitting coefficients are available to users upon request.

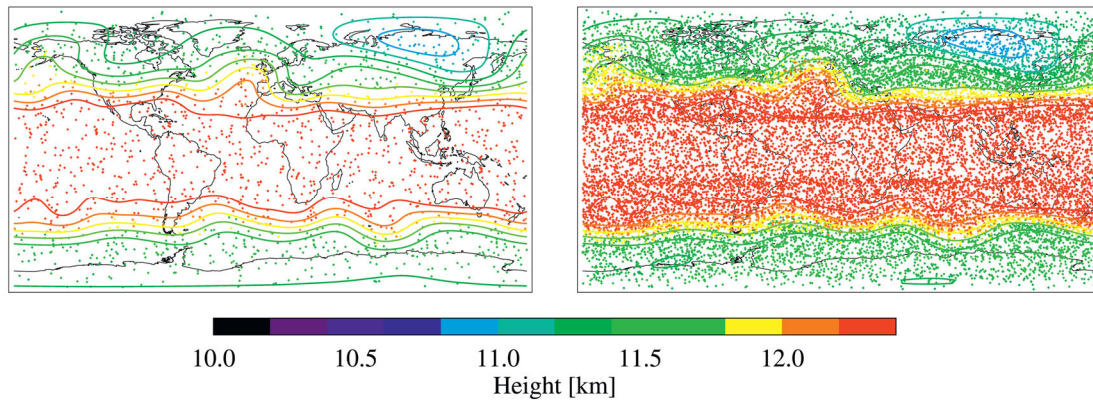


Figure 1. Geopotential height at 200 hPa from 5 days of CHAMP (left) and COSMIC (right) data are optimally fitted using a set of spherical harmonics. Each occultation is represented by a dot. The contours are obtained from the spherical harmonics fit. Please refer to Leroy et al. [2012].

4. Validation and Uncertainty Estimate

The uncertainty estimates obtained here are based on theoretical analyses that have been substantiated through numerous cross-validation studies with radiosondes [Sun et al., 2010] and collocated satellite measurements [e.g., Wang et al., 2004; Schwartz et al., 2008], comparison between RO measurements from different satellites [Hajj et al., 2004; Schreiner et al. 2007], as well as retrieval comparisons among different processing centers [Ho et al., 2012; Steiner et al. 2013].

The uncertainty in the monthly gridded data consists of retrieval and sampling uncertainties. An extensive analysis of the difference sources of retrieval error has been considered in Kursinski et al. [1997]. Some errors, such as those related to horizontal inhomogeneity and local multipath, are expected to be negligible after

spatial and temporal averaging. Other errors, such as those from residual ionospheric bending in the stratosphere and contribution of water vapor at the upper troposphere in the tropics, are systematic and will be present in the monthly gridded data. These systematic error sources are included in the estimates shown in Fig. 2 (black lines labeled “Obs”). These show the characteristic error characteristics for RO retrieval where the best accuracy occurs within 50–250 hPa. We note that these are worst-case estimates corresponding to daytime solar maximum conditions and tropical water vapor values.

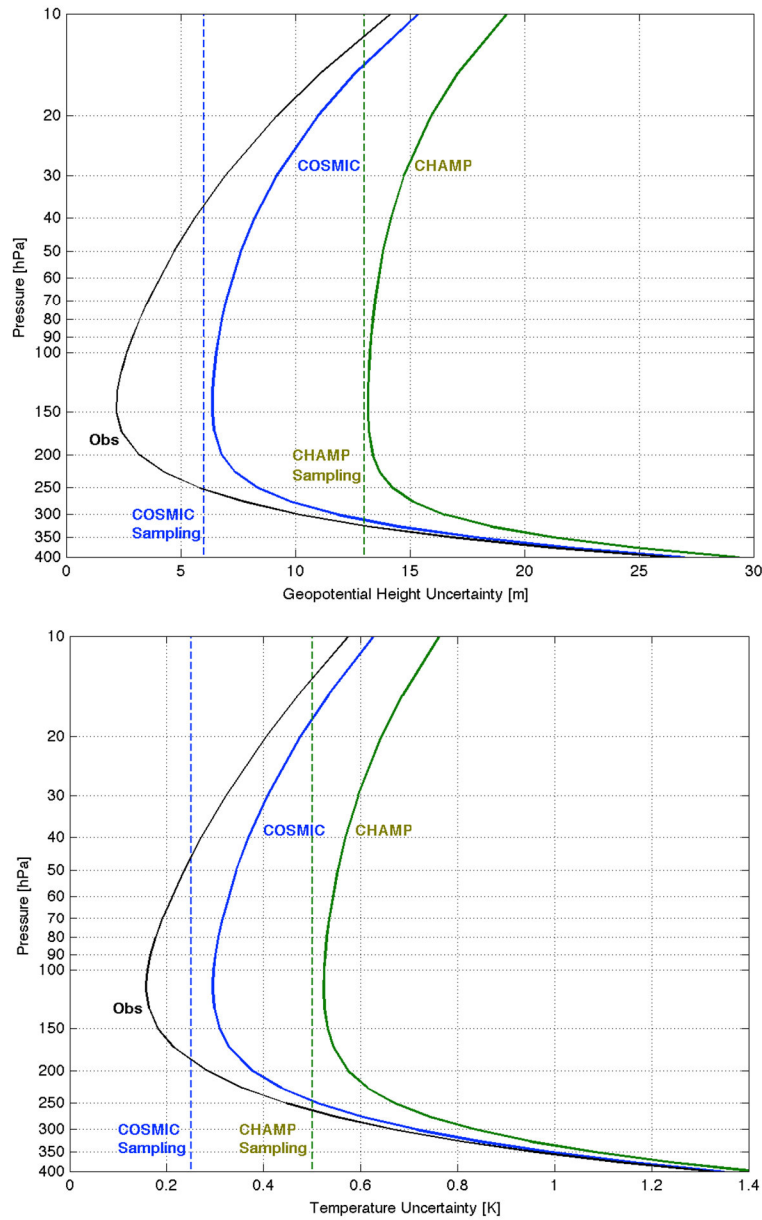


Figure 2. Upper bound error estimates for the monthly gridded geopotential height (top) and temperature (bottom) data from CHAMP (green solid curve) and COSMIC (blue solid curve) in the UTLS. The black solid curves labeled “Obs” represents the retrieval error that does not average out with spatial and temporal averaging. The dashed lines show estimates of sampling errors, with CHAMP (green) having about twice the sampling error of COSMIC (blue).

Sampling error is a significant part of the total uncertainty, especially at the CHAMP measurement density. We estimate the sampling error by generating a synthetic RO dataset based on subsampling ECMWF reanalysis data at RO sounding times and

locations, deriving the monthly gridded dataset with the same algorithm, and comparing against the full reanalysis data [Leroy et al., 2012]. The sampling errors are found to be largest in the middle latitudes and vary weakly with pressure. For simplicity, we will assume that they are constant. Fig. 2 shows the estimated sampling errors in geopotential height and temperature (dashed blue/green lines), where CHAMP sampling errors are about twice as large as COSMIC.

The total uncertainty for the monthly gridded data is obtained by the root-square-sum of the systematic error and the sampling error (solid blue and green lines in Fig. 2 for COSMIC and CHAMP respectively). For a similar approach towards estimating the uncertainty in climatological averages of RO retrievals, please see Scherlin-Pirscher et al. [2011].

5. Considerations for Model-Observation Comparisons

Vertical levels and resolution: The retrieved profiles have a vertical resolution of 200 m below 20 km altitude ($p \geq 50$ hPa) and 1 km above 20 km ($p < 50$ hPa). Therefore, the data between the given pressure levels can be considered uncorrelated.

Sampling change: The dataset comprises data from CHAMP (2002/01–2006/04) and COSMIC (2006/05–2014/12), which have very different sampling characteristics. COSMIC has an order of magnitude more profiles per month than CHAMP. In addition, COSMIC provides good local time coverage each month while CHAMP samples different local times with a repeat cycle of approximately every 4 months. Thus the data from the COSMIC era has a much smaller sampling error than CHAMP in the monthly gridded dataset (cf. Fig. 2).

No Scene-Dependent Sampling bias: Since GPS signals are not significantly affected by clouds or precipitation, we do not expect any sampling bias related to cloud cover or precipitation pattern.

6. Instrument Overview

GPS RO is an active limb sounding technique where radio signals continuously broadcasted by the GPS satellite constellation are tracked by a receiver in a low Earth orbit (Fig. 3). Each RO sounding records the time series of phase delay and signal-to-noise ratio (SNR) of the radio signals transmitted from a GPS satellite as the signal traverses through the different layers of the atmosphere.

At the basic level, the excess Doppler frequency shift of the signal derived from the phase delay, along with precise orbit determination (POD) of the GPS and receiver orbits and clocks, can be directly related to the bending of the signal through the laws of geometric optics and the assumption of local spherical symmetry. The bending angle profile can then be integrated to yield a vertical profile of refractivity as a function of the orthometric height (or geopotential height). Assuming

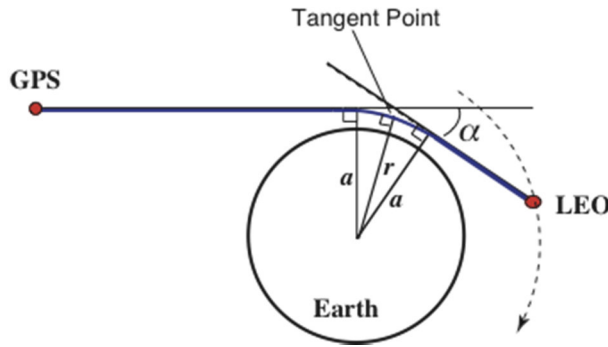


Figure 3. An illustration of the GPS RO observation geometry. A GPS receiver on a low Earth orbit tracks the radio signal transmitted by a GPS satellite and precisely measures the phase delay of the signal passes through the atmosphere. The phase delay measurements are used to infer the bending of the signal, from which the temperature and pressure at the ray tangent point height can be derived.

hydrostatic equilibrium, temperature and pressure can be obtained by integrating the refractivity from some height with an assumed temperature. In this way, we obtain a vertical profile of temperature and geopotential height as a function pressure. More details of the retrieval methodology can be found in Hajj et al. [2002].

The key instrument for RO is the GPS RO receiver that is designed to track carrier phases from the L-band radio signals transmitted by the GPS satellites. Launched in 2000, the CHAMP satellite carried the NASA/JPL BlackJack receiver which is capable of tracking both L1 and the encrypted L2 signal using a codeless tracking technology. Dual-frequency tracking is important for the removal of ionospheric contribution in the retrieved atmospheric profiles. CHAMP was placed in a high-inclination, nearly circular orbit with initial orbital altitude of 454 km. Being in a non-sun-synchronous orbit, the local times of the measurements drift at a rate of ~ 3 hours per month [Pirscher et al., 2007].

Unlike CHAMP, COSMIC was designed to be primarily a GPS RO mission. Launched in 2006, each COSMIC spacecraft carried an enhanced BlackJack receiver known as IGOR (Integrated GPS Occultation Receiver) that was built by Broad Reach Engineering based on JPL design. The IGOR was configured with open-loop tracking functionality that greatly improved lower troposphere tracking. COSMIC consists of six satellites in high-inclination circular orbit with altitudes 700–800 km in separate orbital planes, providing an order-of-magnitude increase in number of soundings and excellent coverage in diurnal cycle [Xie et al. 2010]. A number of spacecraft issues have degraded the performance of the constellation, leading to a $\sim 20\%$ drop in throughput starting in 2010.

7. References

- NASA/JPL Global Environmental & Earth Science Information System (GENESIS) portal, <http://genesis.jpl.nasa.gov>.
 Anthes, R. A., et al. (2008), The COSMIC/FORMOSAT-3 mission: Early results, *Bull. Am. Meteorol. Soc.*, 89, 313–333.

- Hajj, G. A., E. R. Kursinski, L. J. Romans, W. I. Bertiger, and S. S. Leroy (2002), A technical description of atmospheric sounding by GPS occultation, *J. Atmos. Sol. Terr. Phys.*, 64(4), 451–469, doi:10.1016/S1364-6826(01)00114-6.
- Hajj, G. A., C. O. Ao, B. A. Iijima, D. Kuang, E. R. Kursinski, A. J. Mannucci, T. K. Meehan, L. J. Romans, M. de la Torre Juarez, and T. P. Yunck (2004), CHAMP and SAC-C atmospheric occultation results and intercomparisons, *J. Geophys. Res.*, 109, D06109, doi:10.1029/2003JD003909.
- He, W., S.-P. Ho, H. Chen, X. Zhou, D. Hunt, and Y.-H. Kuo (2009), Assessment of radiosonde temperature measurements in the upper troposphere and lower stratosphere using COSMIC radio occultation data, *Geophys. Res. Lett.*, 36, L17807, doi:10.1029/2009GL038712.
- Ho, S., et al. (2012), Reproducibility of GPS radio occultation data for climate monitoring: Profile-to-profile intercomparison of CHAMP climate records 2002 to 2008 from six data centers, *J. Geophys. Res.*, 117, D18111, doi:10.1029/2012JD017665.
- Kursinski, E. R., G. A. Hajj, J. T. Schofield, R. P. Linfield, and K. R. Hardy (1997), Observing Earth's atmosphere with radio occultation measurements using the Global Positioning System, *J. Geophys. Res.*, 102(D19), 23,429–23,465.
- Leroy, S. S., C. Ao, and O. P. Verkhoglyadova (2012), Mapping GPS radio occultation data by Bayesian interpolation, *J. Atmos. Oceanic Technol.*, 29, 1062–1074, doi:10.1175/JTECH-D-11-00179.1.
- Pirscher, B., U. Foelsche, B. C. Lackner, and G. Kirchengast (2007), Local time influence in single-satellite radio occultation climatologies from Sun-synchronous and non-Sun-synchronous satellites, *J. Geophys. Res.*, 112, D11119, doi:10.1029/2006JD007934.
- Scherllin-Pirscher, B., G. Kirchengast, A. K. Steiner, Y.-H. Kuo, and U. Foelsche (2011), Quantifying uncertainty in climatological fields from GPS radio occultation: an empirical-analytical error model, *Atmos. Meas. Tech.*, 4, 2019–2034.
- Schreiner, W., C. Rocken, S. Sokolovskiy, S. Syndergaard, and D. Hunt (2007), Estimates of the precision of GPS radio occultations from the COSMIC/FORMOSAT-3 mission, *Geophys. Res. Lett.*, 34, L04808, doi:10.1029/2006GL027557.
- Schwartz, M. J., et al. (2008), Validation of the Aura Microwave Limb Sounder temperature and geopotential height measurements, *J. Geophys. Res.*, 113, D15S11, doi:10.1029/2007JD008783.
- Steiner, A. K., et al. (2013), Quantification of structural uncertainty in climate data records from GPS radio occultation, *Atmos. Chem. Phys.*, 13, 1469–1484.
- Sun, B., Reale, A., Seidel, D. J., and Hunt, D. C. (2010), Comparing radiosonde and COSMIC atmospheric profile data to quantify differences among radiosonde types and the effects of imperfect collocation on comparison statistics, *J. Geophys. Res.*, 115, D23104, doi:10.1029/2010JD014457.
- Wang, D.-Y., et al. (2004), Cross-validation of MIPAS/ENVISAT and GPS-RO/CHAMP temperature profiles, *J. Geophys. Res.*, 109, D19311, doi:10.1029/2004JD004963.
- Wickert, J., et al. (2001), Atmospheric sounding by GPS radio occultation: first results from CHAMP, *Geophys. Res. Lett.*, 28(17), 3263–3266.

Xie, F., D. L. Wu, C. O. Ao, and A. J. Mannucci (2010), Atmospheric diurnal variations observed with GPS radio occultation soundings, *Atmos. Chem. Phys.*, 10, 6889–6899.

8. Dataset and Document Revision History

Rev 0 – 1 Jun 2016 - This is a new document/dataset